0022-1554/91/$3.30
The Journal of Histochemistry and Cytochemistry

Vol. 39, No. 9, pp. 1267–1279, 1991
Printed in U.S.A.

Brief Report

Freeze-substitution and Lowicryl HM20 Embedding of Fixed Rat Brain: Suitability for Immunogold Ultrastructural Localization of Neural Antigens

MENNO VAN LOOKEREN CAMPAGNE, A. BEATE OESTREICHER,[1] THEO P. VAN DER KRIFT, WILLEM HENDRIK GISPEN, and ARIE J. VERKLEIJ

Department of Pharmacology, Rudolf Magnus Institute and Institute of Molecular Biology (MVLC,ABO,WHG), and Department of Molecular Cell Biology (TPK,AJV), University of Utrecht, 3584 CH Utrecht, The Netherlands.

Received for publication January 24, 1991 and in revised form April 26, 1991; accepted May 6, 1991 (1B2217).

We examined the suitability of freeze-substitution and Lowicryl HM20 embedding of aldehyde-fixed rat brain to localize several neural antigens at the ultrastructural level. The following rabbit polyclonal and mouse monoclonal antibodies were used: affinity-purified polyclonal immunoglobulins G raised to B-50/GAP43 (a membrane-anchored, growth-associated protein); affinity-purified polyclonal immunoglobulins G to human glial fibrillary acidic protein (GFAP; a subunit of glial filaments); a polyclonal antiserum raised to adrenocorticotropic hormone[25–39] (a neuropeptide present in dense-core granules); a polyclonal antiserum raised to myelin basic protein (a protein present in compact myelin of the central nervous system); and mouse monoclonal antibodies to synaptophysin (an integral membrane protein of small synaptic vescicles). Rat mesencephalon was fixed by perfusion with buffered 2% glutaraldehyde and 4% paraformaldehyde, cryoprotected, and frozen in liquid nitrogen. Freeze-subsitution of tissue was performed with anhydrous methanol and 0.5% uranyl acetate at −90°C. Semithin Lowicryl sections were used for light microscopic visualization of B-50 in the ventromedial mesencephalic central gray substance. The procedure preserves well the ultrastructure of this region and the immunoreactivity of the selected antigens. This study shows that dehydration by freeze-substitution, combined with Lowicryl HM20 embedding at sub-zero temperature, provides a successful method of preparation of fixed brain tissue for ultrastructural studies, allowing immunogold localization of several neural antigens by double labeling in the same section and in serial sections. (*J Histochem Cytochem 39:1267–1279, 1991*)

KEY WORDS: Rat brain; Mesencephalic central gray substance; Freeze-substitution; Lowicryl HM20; Immunogold labeling; B-50/GAP43; GFAP; Ultrastructure; Electron microscope.

Introduction

Immunogold labeling of neural antigens in ultra-thin cryosections of brain tissue has been performed successfully in several studies (6,41). Ultrastructure and antigenicity in melted cryosections are adequately preserved, but integrity of the sections is too low to obtain serial sections and large sections for overviews (19). Therefore, immunodetection of relatively scarce neuronal elements, e.g., such as in the mesencephalic central gray substance (MCG), the varicosities containing adrenocorticotropic hormone (ACTH), and the cell bodies of astrocytes, is hard to carry out in cryosections. Suitable sectioning properties can be obtained when tissues are embedded in resins. This procedure entails osmium fixation, dehydration at room temperature, and embedding in epoxy resin, a standard method that guarantees sufficient preservation of ultrastructure in ultra-thin sections of brain tissue. However, many neuronal antigens such as B-50, synaptophysin (p38), glial fibrillary acidic protein (GFAP), and myelin basic protein (MBP) show virtually no immunoreactivity after osmium fixation and epon embedding. Omission of osmium fixation results in deleterious structural effects when the tissue is dehydrated by the organic solvents at room temperature before resin embedding and polymerization at 60°C. Controlled dehydration and embedding of non-osmium-fixed tissue with structural preservation is possible at sub-zero temperatures. For this purpose, resins have been developed that are suitable for embedding biological specimens at temperatures ranging from −30°C to −50°C. The resins can subsequently be polymerized by UV light at temperatures ranging from −45°C to −85°C (4,5). The polar K4M and the non-polar HM20 Lowicryl resins have become well established within the use of the progressive lowering of temperature (PLT) method carried out by dehydrating chemically fixed specimens in organic solvents while the temperature is progressively lowered (4). Lowicryl K4M has also been applied to embed brain tissue at room temperature after dehydration at −4°C (37). However, the temperatures used during dehydration of the tissues with these techniques are not sufficiently low to prevent loss of lipids

[1] Correspondence to: Dr. A.B. Oestreicher, Institute of Molecular Biology and Medical Biotechnology. University of Utrecht, Padualaan 8, 3584 CH Utrecht, The Netherlands.

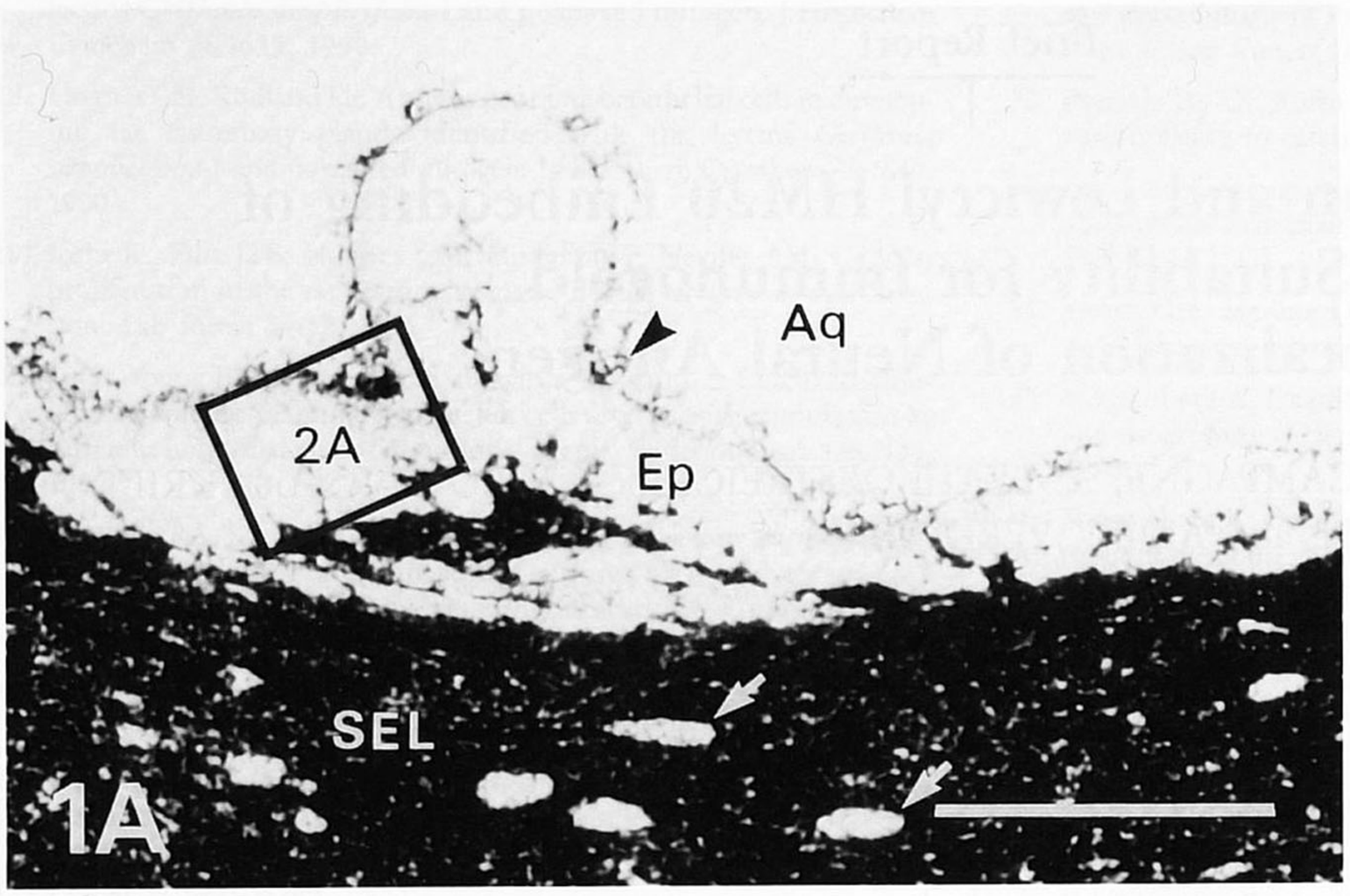

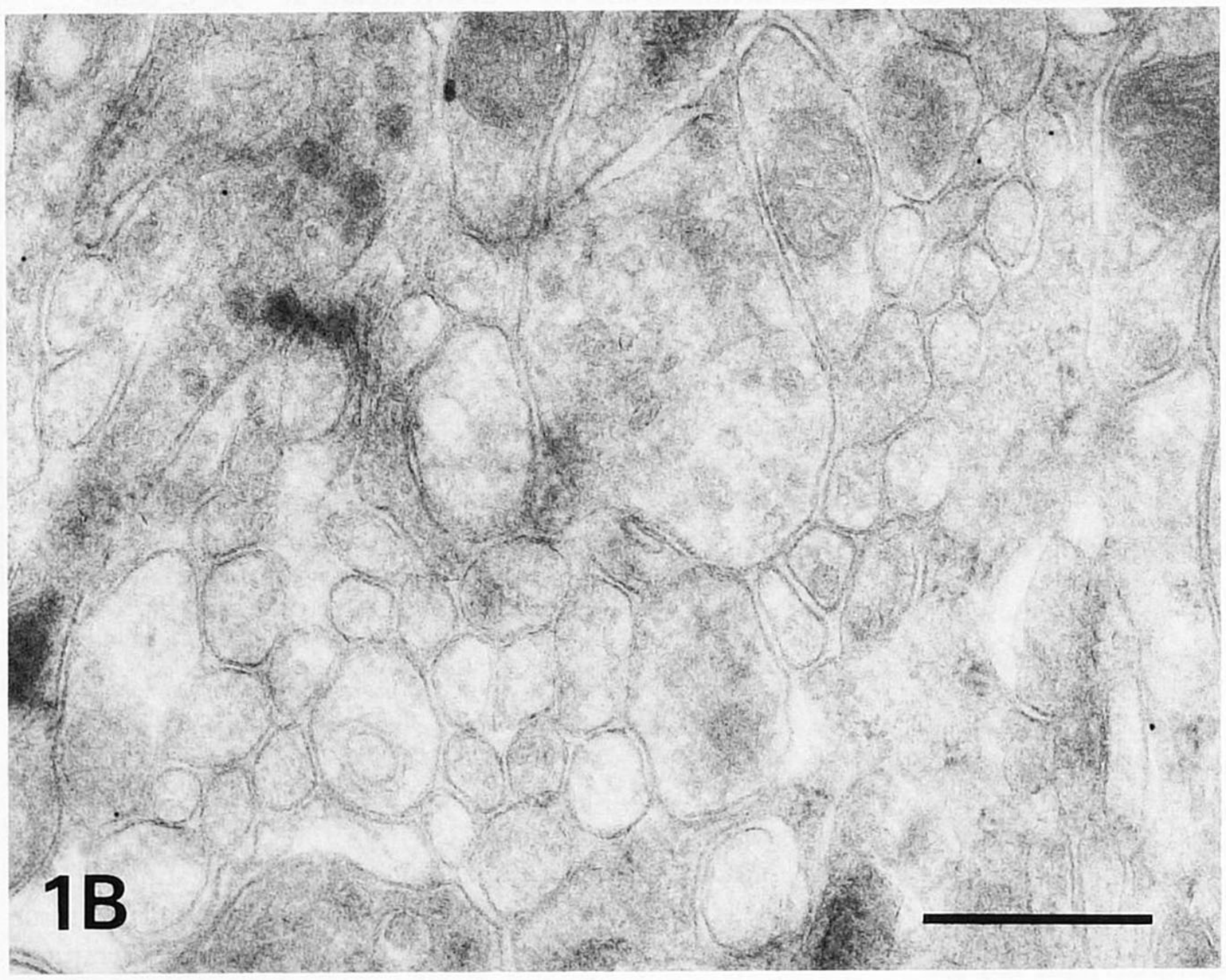

Figure 1. (**A**) Light micrograph of semi-thin (0.5 μm) Lowicryl section through ependymal thickening of the ventricular wall of the aqueduct (Aq) in the mesencephalic central gray substance (MCG). B-50 antibodies are visualized by silver enhancement of 1-nm gold particles coated with goat anti-rabbit IgGs. B-50 immunoreactivity is present in the supra-ependymal plexus (arrowhead) at the ventricular border of the ependymal cells (Ep) and in the neuropil of the sub-ependymal layer (SEL). The ependymal cells and cell bodies in the sub-ependymal region of the MCG (white arrows) are devoid of B-50 immunoreactivity. Electron micrographs of the framed area are shown in Figure 2. (**B**) Control electron micrograph of ultra-thin Lowicryl section of the MCG incubated with pre-immune IgGs and 10-nm gold particles coated with goat anti-rabbit IgGs. Bars: **A** = 50 μm; **B** = 0.5 μm.

Figure 2. Electron micrographs of ultra-thin sections of the ventricular border of the MCG immunoreacted with anti-B-50 IgGs and detected with goat anti-rabbit IgGs coupled to 10-nm gold particles. The sections were taken adjacent to the semi-thin section shown in Figure 1A. (**A**) Low-power micrograph of the ependymal thickening. BV, blood vessel. (**B**) Detail of the supra-ependymal plexus, framed in **A**. Note the varicose appearance of these fibers, which contain dense-core vesicles (open arrow). The electron micrographs clearly show that the plasma membranes of supra-ependymal fibers (arrowheads) are highly immunoreactive for B-50. B-50 immunoreactivity is also found in the cytosol of these fibers, and appears to be present at some of the dense-core granules. The cilia (stars) show lower but still a significant amount of B-50 immunoreactivity, but the apical membranes of the ependymal cells (curved arrows) are without B-50 immunoreactivity. (**C**) Part of the subependymal layer with longitudinally sectioned unmyelinated axons (Ax), containing high B-50 immunoreactivity at their plasma membranes. Bars: **A** = 5 μm; **B**,**C** = 0.5 μm.

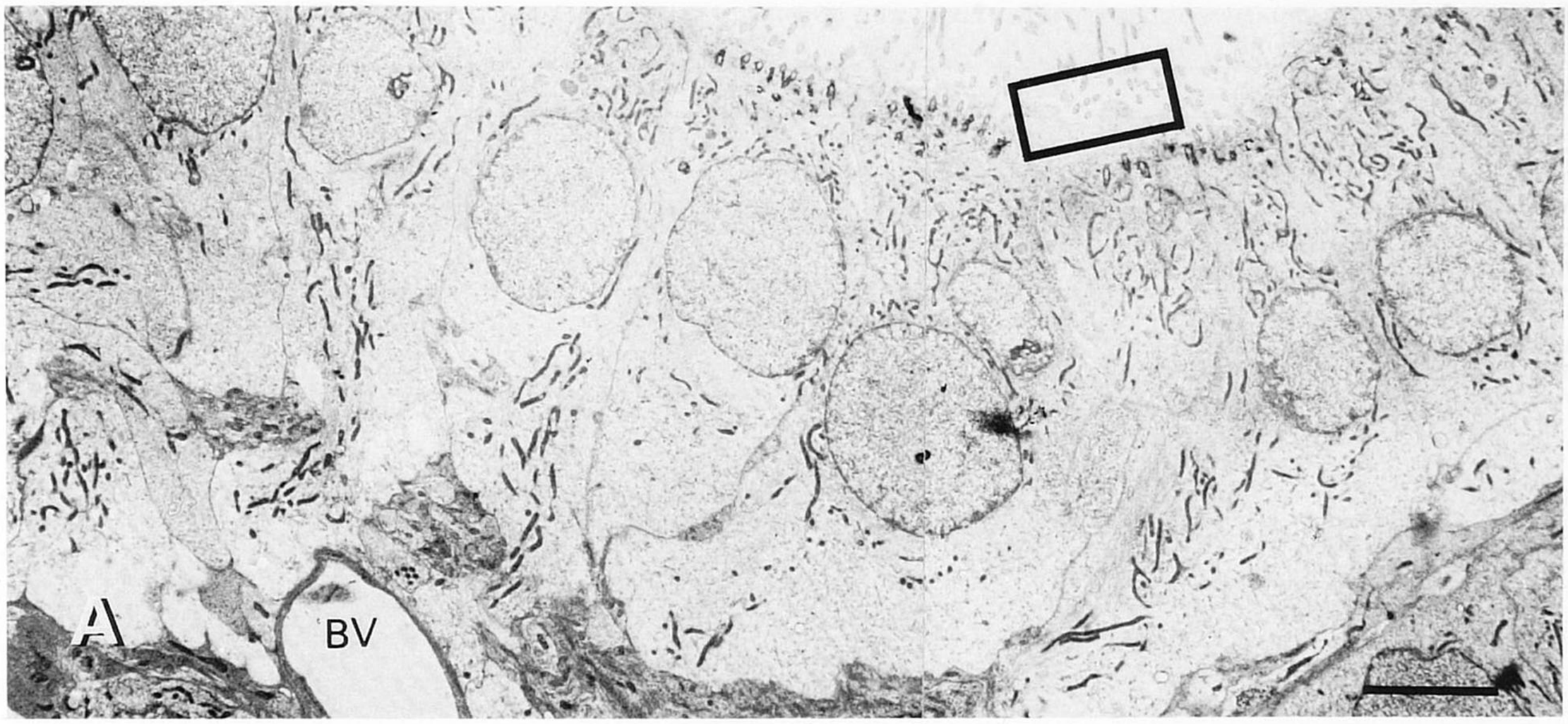
A
BV

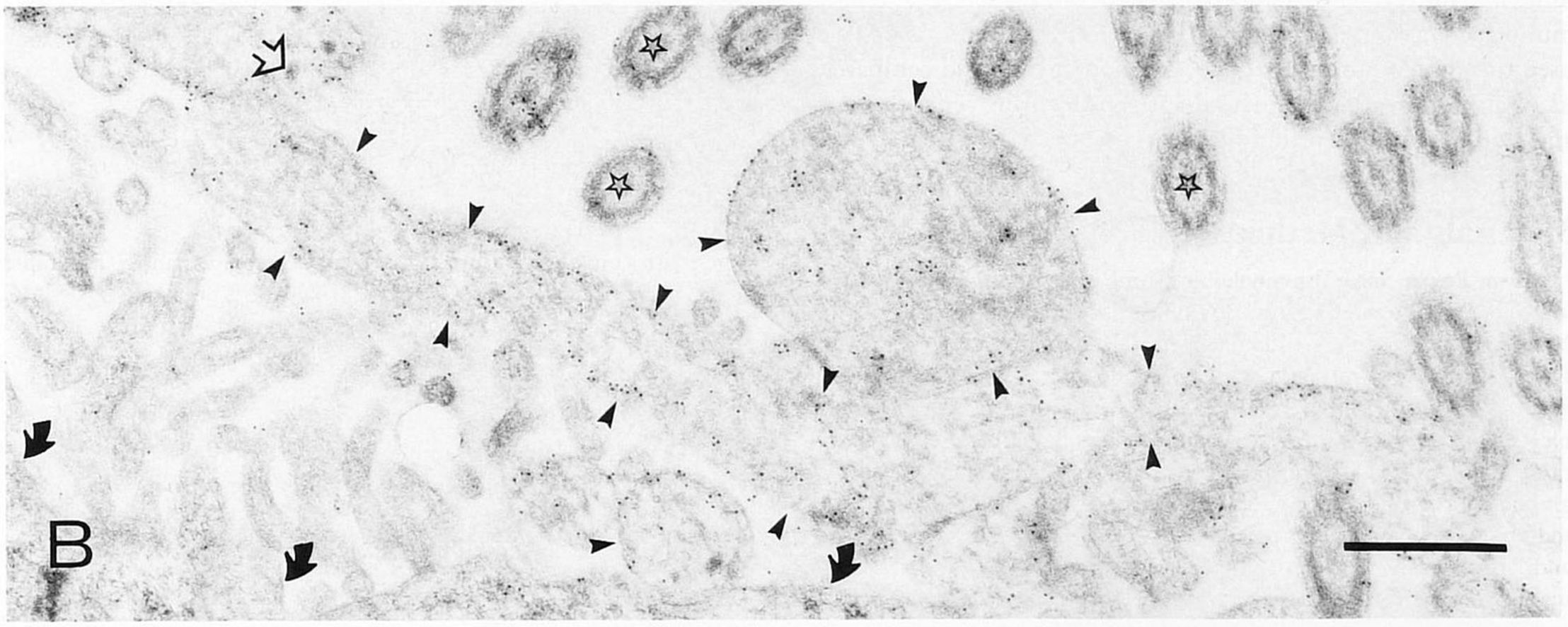
B

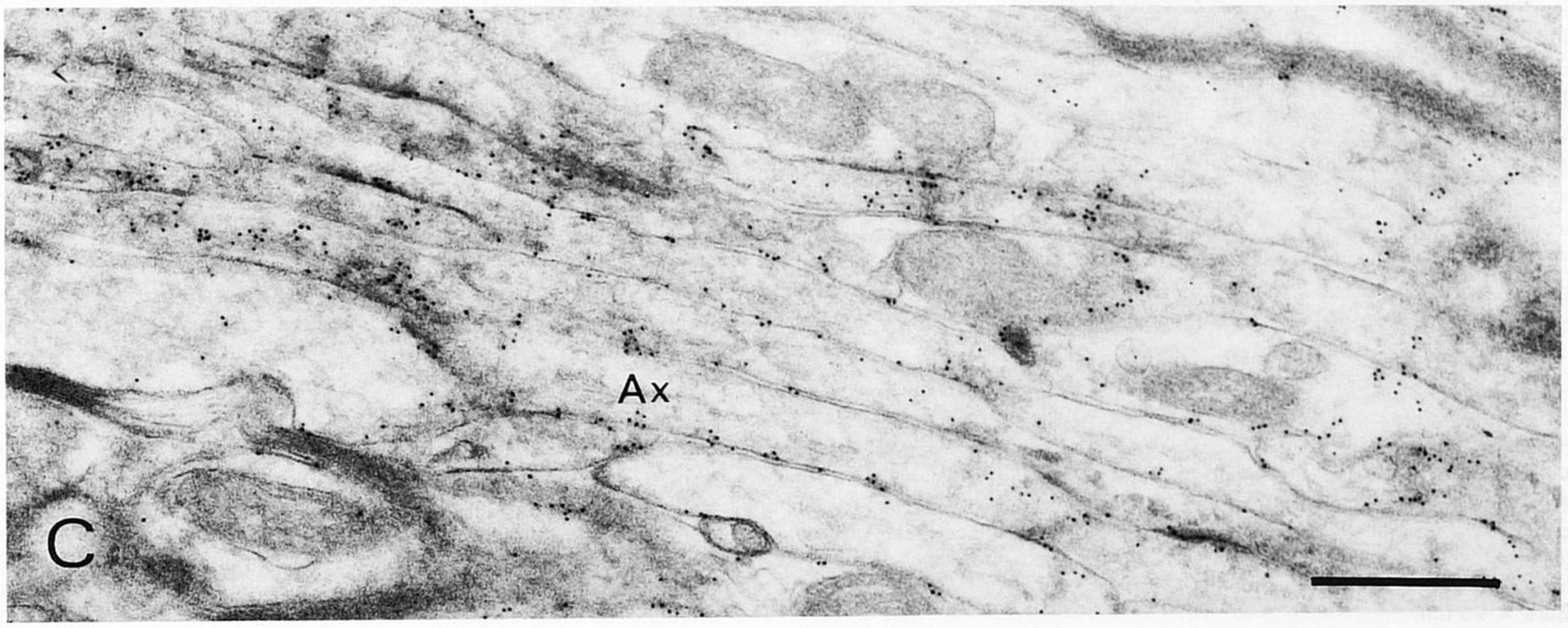
Ax
C

Table 1. *Assessment of antibody specificity by quantitation of gold particle density over various cellular elements in the mesencephalic central gray substance*[a]

Antibodies to	Ax	AT	MAx	As	Den	Mit
B-50	69.4 ± 4.6 (20)*	—	—	2.2 ± 0.9 (5)	6.9 ± 1.6 (8)	10.6 ± 2.9 (19)
SY38	—	187.7 ± 24.0 (9)*	—	—	26.3 ± 5.9 (10)	74.6 ± 12.5 (11)
MBP	0.5 ± 0.5 (6)	—	204.5 ± 23.3 (8)*	—	—	3.4 ± 2.4 (8)
GFAP	0.3 ± 0.2 (11)	—	—	169 ± 1 (11)*	—	3.6 ± 1.8 (11)
ACTH	0.7 ± 0.3 (9)	44.6 ± 8.4 (9)*#	—	—	—	9.6 ± 4.7 (17)

[a] Values represent mean number of gold particles/μm^2 ± SEM measured over (n) segments of various cellular elements in ultra-thin Lowicryl sections, incubated with antibodies raised against different antigens. Ax, unmyelinated axons; AT, axon terminal; MAx, myelinated axon; As, astrocyte; Den, dendrite; Mit, mitochondrion. High SEM values relative to the mean value in some cases are due to the absence of gold particles in almost all quantitated segments. #, gold particle density in ACTH-immunoreactive varicosities. Asterisks indicate values significantly different ($p<0.001$) compared with other values in the same row (Student's t-test).

and denaturation of proteins, resulting in reduced ultrastructural preservation and antigen–antibody binding (13,30). These negative effects of the organic solvent can be limited by freezing aldehyde-fixed, cryoprotected specimens in liquid propane and dehydrating in methanol at −90°C in the presence of 0.5% uranyl acetate as the stabilizing agent (13,30). In the present study, we show that this method of dehydration combined with low-temperature embedding in Lowicryl HM20 preserves both ultrastructure and immunoreactivity of selected neural antigens in rat brain tissue. We used this method to study the localization of B-50 and compared its localization with other neural antigens by using serial sections and double labeling techniques.

Materials and Methods

Tissue Preparation. Thromboliquine (1 ml/kg body weight) was injected intravenously into three adult male albino rats (Wistar strain, body weight 230–250 g) which were anesthetized with Narcovet (Apharmo; Arnhem, The Netherlands) (1 ml/kg body weight). The rats were perfused through the left ventricle of the heart with 0.9% (w/v) NaCl until the liver was bleached. Perfusion was continued with 250 ml of a freshly prepared solution of 4% (w/v) paraformaldehyde (BDH; Poole, UK) and 2% (w/v) glutaraldehyde (biological grade; Polysciences, Warrington, PA) in 0.1 M sodium phosphate buffer at pH 7.4 (PB), 37°C. The brains were dissected and left overnight in fixative at 4°C, followed by storage in 1% paraformaldehyde in PB until the time of processing.

Freeze-substitution and Low-temperature Embedding. Coronal sections 100 µm thick were cut from the MCG in PB at 4°C with a vibratome (Micro-Cut H1200; Bio-Rad Microscience Division, Watford, Hertfordshire, UK). The area of study corresponds to coordinate Bregma −8.0 according to the atlas of Paxinos and Watson (26). To prevent antibody binding to aldehyde groups of the fixative during the immunoincubations, the sections were treated with 0.1% (w/v) sodium borohydride and 50 mM glycine in PB. Tissue sections were cryoprotected by immersion in increasing concentrations of glycerol (10–20–30%, v/v) in PB, 0.5 hr for each concentration. Triangular pieces of the mediobasal area of the MCG were dissected from the vibratome sections (100 µm thick) with a razor blade and oriented on circular pieces of Thermanox (Lab-Tek Div., Miles Laboratories; Naperville, IL) with a diameter of 4 mm. Oval one-hole grids were placed on top of the Thermanox and the pieces of tissue were oriented in the hole. A copper cover was placed on top of the grid. The sandwiched tissue was clamped with a forceps and plunged into liquid propane cooled by liquid nitrogen (−190°C), using a rapid-freeze apparatus (KF80; Reichert–Jung, Wien, Austria). After freezing, the copper cover was removed and the specimen was transferred to the pre-cooled chamber (−90°C) of a CS auto, freeze-substitution apparatus (Reichert–Jung). Freeze-substitution was done as described by Müller et al. (22). The tissue was immersed overnight in anhydrous methanol at −90°C, containing 0.5% (w/v) uranyl acetate as fixing agent. The temperature was raised stepwise with a 4°C increment per hour from −90°C to −45°C. The samples were washed several times with anhydrous methanol to remove residual water and excess uranyl acetate before infiltration with Lowicryl HM20 resin (Chemische Werke Lowi; Waldkraiburg, FRG). The embedding process was carried out at −45°C in three stages, with a progressively increasing ratio of resin to methanol. The samples were transferred to an embedding mall filled with pure resin at −45°C. The resin was subsequently polymerized overnight at −45°C, catalyzed by UV radiation (360 nm) emitted from a source at the top of the embedding mall. The polymerized samples were taken out of the mall and exposed to diffuse UV radiation for 1 day at room temperature. Thin sections were cut on a Reichert Ultramicrotome OM3 and mounted on formvar- and carbon-coated oval one-hole nickel grids.

Antibodies. The antiserum to ACTH [25–39] was raised in rabbits against synthetic porcine ACTH [25–39] (Ciba Ceigy; Basel, Switzerland) conjugated with human bovine serum albumin. This antiserum was a gift of Dr. A.A.J. Verhofstad. The specificity of the anti-ACTH [25–39] antiserum has been confirmed (7,35,39).

Production, characterization, and affinity-purification of rabbit polyclonal antibody to B-50 have been described in detail (24,25). Specificity of the antibodies to B-50 (code 8613) has been extensively tested in previous electron microscopic studies (41,42). Rabbit immunoglobulins G (IgGs) directed against cow glial fibrillary acidic protein (anti-GFAP) and rabbit serum against human myelin basic protein (anti-MBP) were obtained from Dakopatts (Glostrup, Denmark). Mouse monoclonal antibodies (MAb) against synaptophysin (clone SY38) were obtained from Boehringer (Mannheim, FRG). The antibodies were used in the following dilutions: 1:75 for

Figure 3. (**A**) Overview and (**B**) detail of ultra-thin Lowicryl section immunoincubated with anti-B-50 IgGs and goat anti-rabbit IgGs coupled to 10-nm gold particles. The section was obtained from the basolateral region of the MCG, more distal from the aqueduct compared with Figure 2. Open star indicates a varicosity that contains electron-lucent small synaptic vesicles (SSV) only; closed star indicates a varicosity containing a mixed population of SSV and large dense-core vesicles (DCV). The plasma membranes of cross-sectioned small unmyelinated axons (Ax) show high immunoreactivity, whereas the plasma membrane of a dendrite (Den) is virtually free of B-50 immunoreactivity. The varicosities show B-50 immunoreactivity both at their plasma membranes and in the cytosol. Mit, mitochondrion. Bars = 0.5 µm.

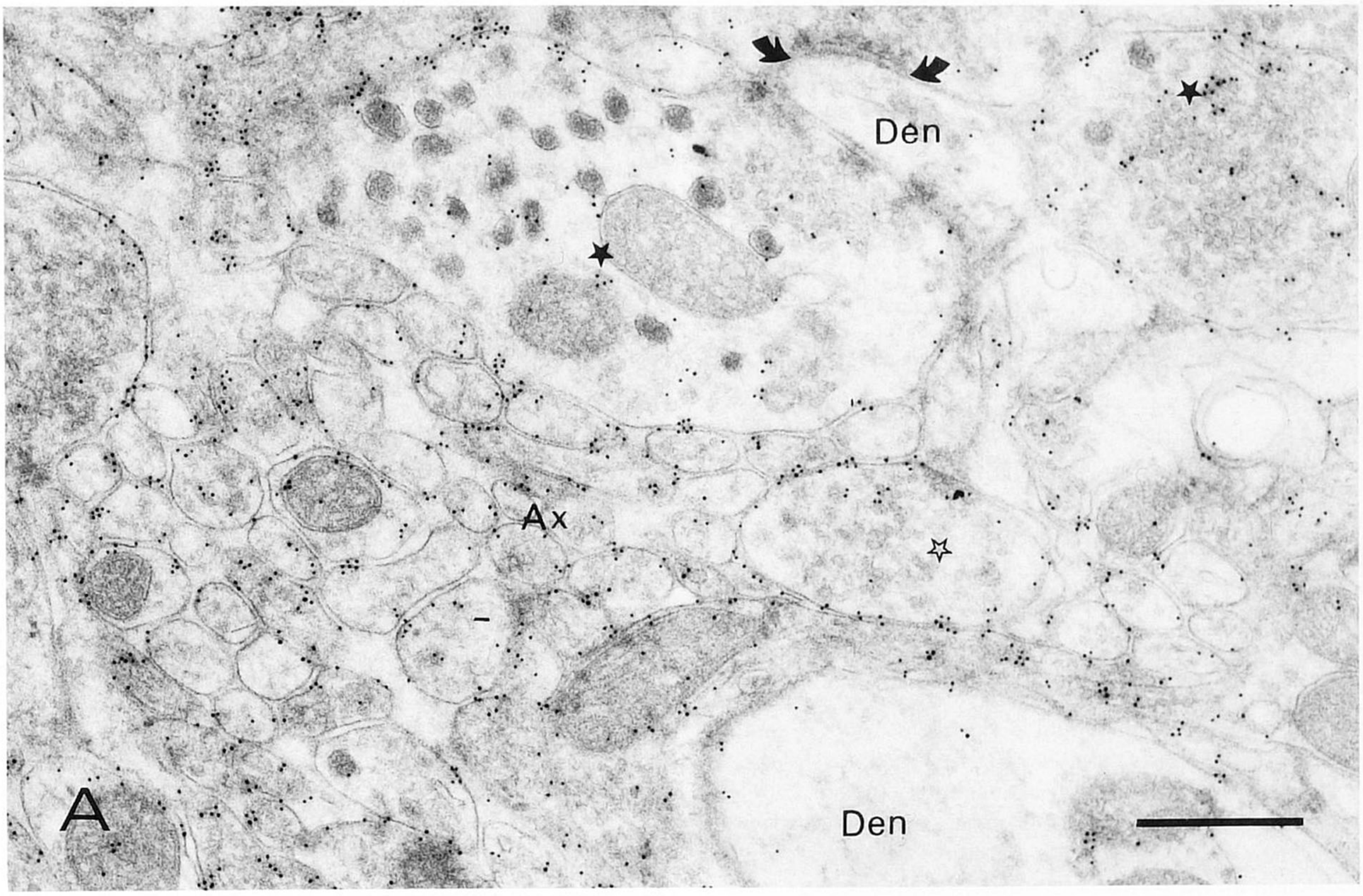
Den
Ax
Den
A

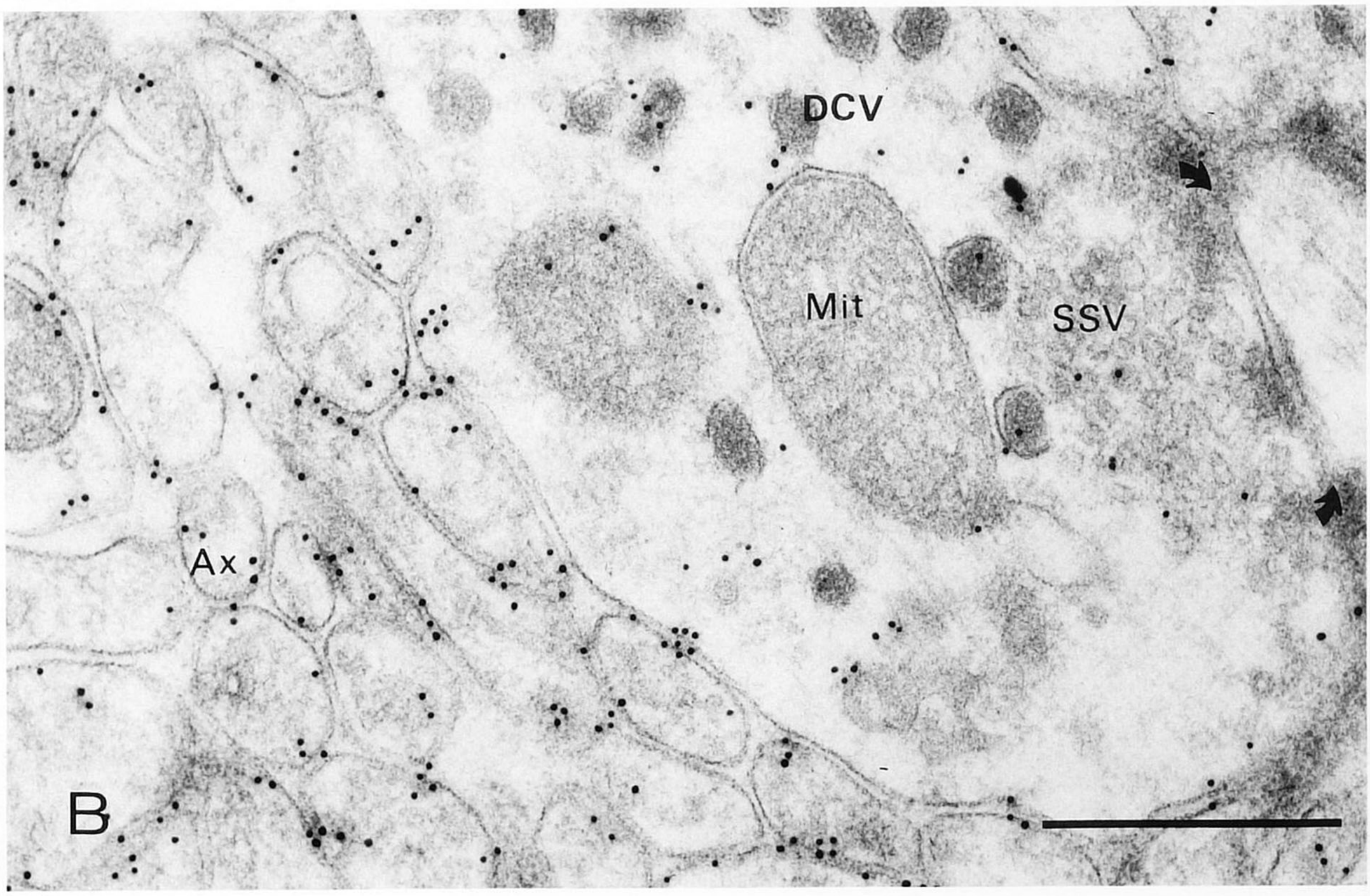
DCV
Mit
SSV
Ax
B

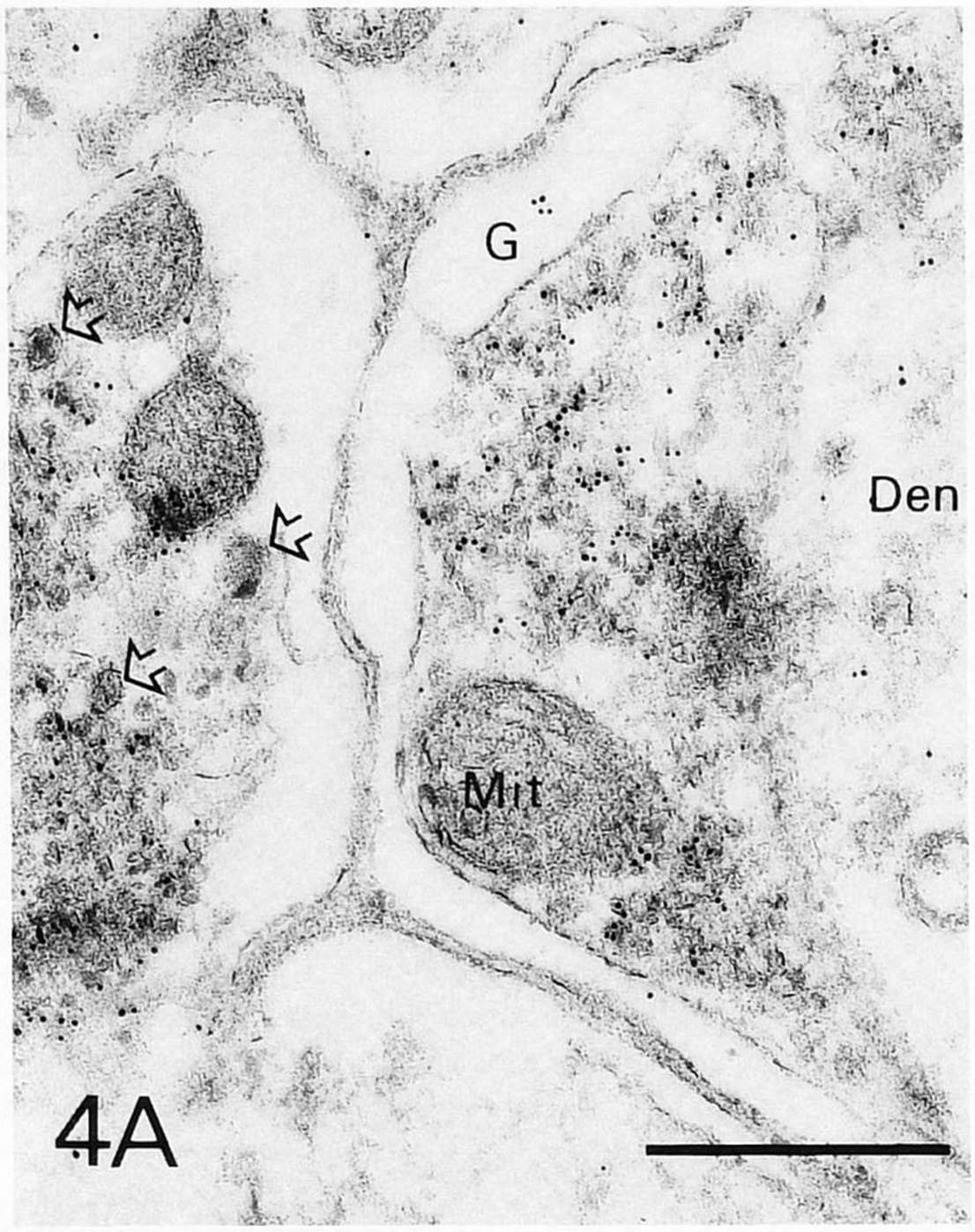

4A

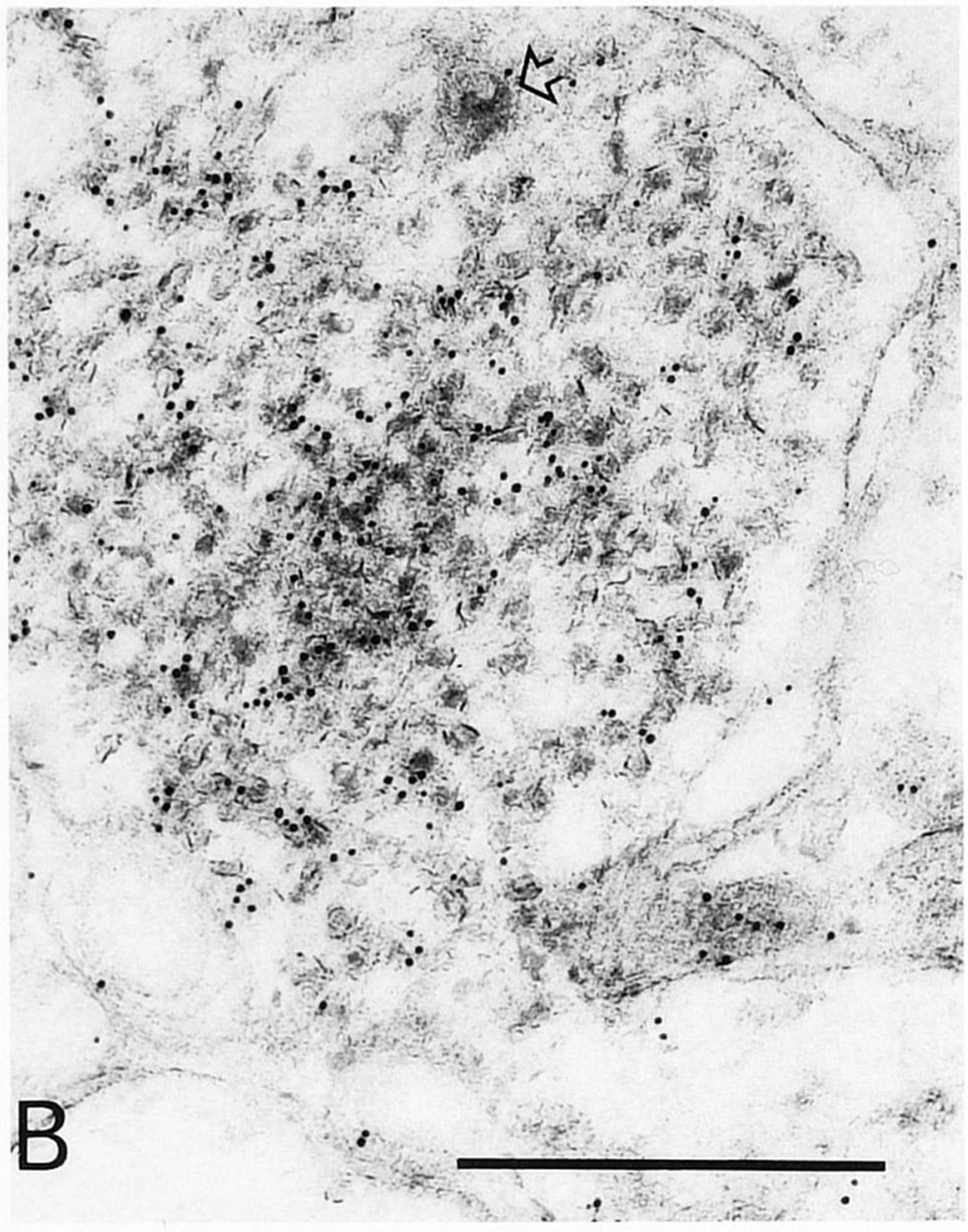

B

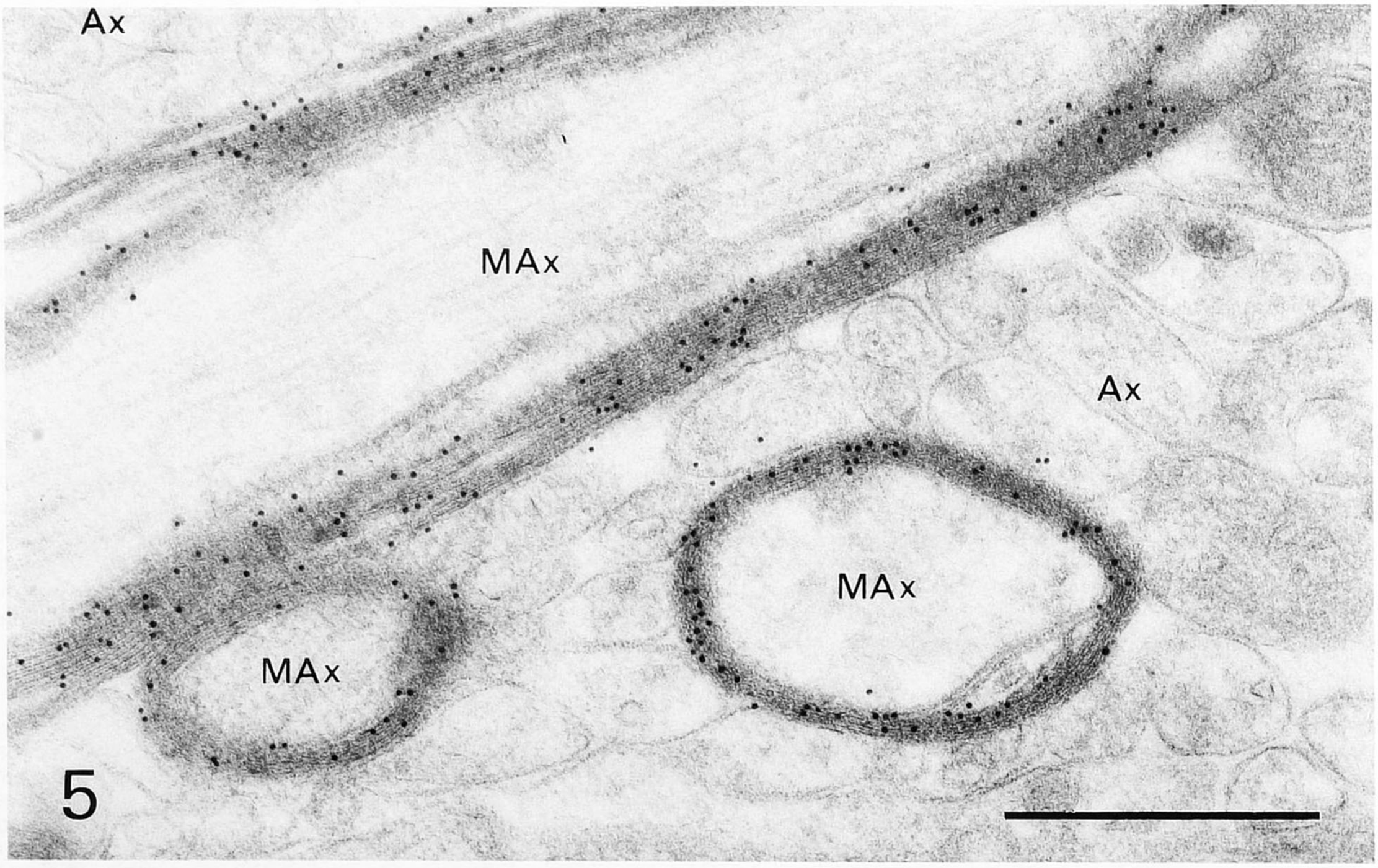

5

anti-B-50 IgGs; 1:100 for anti-MBP serum; 1:750 for anti-ACTH [23–39]; 1:15 for anti-GFAP IgGs; and 1:5 for MAb against synaptophysin supplied as purified IgGs of ascites. The antibodies were freshly diluted before immunoincubation.

Light Microscopy. Lowicryl sections of 500 nm, attached to poly-L-lysine- or gelatin-coated coverslips, were fixed in 2.5% (w/v) glutaraldehyde for 10 min to cross-link the poly-L-lysine or gelatin and washed in PB. The immunoincubation procedure was carried out with antibodies to B-50 and 1-nm gold (Nanoprobe; Janssen Pharmaceutica, Beerse, Belgium) coupled to goat anti-rabbit (GAR) IgGs. The gold particles were silver enhanced for 15 min with the IntenSE silver enhancement kit (Janssen Life Sciences Products; Olen, Belgium) and photographed.

Immunogold Labeling of Ultra-thin Sections. All steps, except for the antibody incubation overnight, were performed at room temperature. Ultra-thin Lowicryl sections from the MCG were washed for 10 min in PB containing 0.1% (w/v) sodium borohydride and 50 mM glycine, and for 10 min in PB containing 0.5% (w/v) BSA and 0.1% (w/v) gelatin (PB + BSA + gelatin = PBG). For single immunolabeling, sections were incubated overnight at 4°C in 4-µl drops of PBG containing the antibodies in dilutions as reported above. Sections were washed 20 min in PBG and incubated in second antibodies attached to gold particles (Janssen Pharmaceutica). For double labeling of ACTH and B-50, sections were first immunostained for ACTH as described for single immunolabeling and washed thoroughly in bi-distilled water. Thereafter, the 10-nm gold particles were silver enhanced for 8–10 min with IntenSE. The diameter of the silver-enhanced particles ranged from 30–80 nm. After the silver enhancement, the sections were washed three times in double-distilled water, twice in PBG, and immunostained for B-50 with GAR IgGs attached to 10-nm gold particles as described for single immunostaining. Sections were contrasted in a saturated solution of aqueous uranyl acetate and lead citrate according to Reynolds (27) and examined with a Philips CM10 electron microscope. As a control, sections were incubated in pre-immune rabbit IgGs. In addition, the method and antibody specificity were tested by counting and comparing the number of gold particles over cell structures in which the antigen is known to be present with the number of gold particles over structures where no specific immunogold labeling is expected. The gold particle density in the cell organelles was determined by video imaging of EM negatives, using a CCD-Sony Video-8 camcorder, an IBM-compatible personal computer, a frame grabber (PCVisionplus; Imaging Technology, Woburn, MA), and a command file (written in TIM version 3.35; DIFA Measuring Systems; Breda, The Netherlands) (unpublished data).

Results

Light Microscopy

Lowicryl embedding of tissue allows light microscopy of silver-enhanced, immunogold-labeled semi-thin sections. This can help to orientate the specimen and is useful for determining the specificity of the antibodies. Figure 1A shows an example of the light microscopic visualization of B-50, showing an ependymal thickening in the ventricular wall of the MCG aqueduct (Aq). High B-50 immunoreactivity is found at the ventricular border of the ependymal cells, probably associated with the supra-ependymal plexus (arrowhead) and throughout the sub-ependymal layer (SEL). The non-neuronal ependymal cell layer (Ep) is clearly devoid of B-50, as are the cell bodies in the sub-ependymal area (white arrows). Electron micrographs of the framed area are shown in Figure 2.

Ultrastructure of the Mesencephalic Central Gray Substance

Figures 1B to 7 show that the preservation of subcellular organelles in the Lowicryl HM20 embedded MCG is of good quality, and the ultrastructure obtained is comparable to that of the osmium-fixed and Epon-embedded MCG (2). Of special importance is the good preservation of microfilaments, e.g., fibrils in astrocytes. Owing to the fair sectioning properties of the polymerized Lowicryl HM20, large sections as well as serial sections can be processed for subsequent immunocytochemical analysis. This enabled us to study comparatively the localization of several antigens with immunogold techniques, applying different specific antibodies on serial sections.

Specificity of the Antibodies and Method of Detection

Substitution of pre-immune IgGs for the primary antibodies results in almost complete absence of immunogold labeling in ultra-thin Lowicryl sections (Figure 1B). Gold particle density in these sections is less than 1 gold particle/µm^2 (n = 15). Gold particle density over empty resin in ultra-thin sections treated with the primary and secondary antibody is less than 0.5 gold particles/µm^2. To get a global impression of the specificity of the immunolabeling, gold particle density over cell elements containing the antigen to which the antibody was raised is compared to the gold particle density in cell elements that are not likely to contain the antigen (Table 1). For all antibodies, gold particle density in cell elements containing the antigen is significantly higher ($p<0.001$) compared with gold particle density due to nonspecific binding of the antibodies (Student's t-test). The ratio of specific to nonspecific immunogold labeling is highest for antibodies to MBP and lowest for antibodies to SY38.

Immunogold Labeling of B-50, Synaptophysin, and Myelin Basic Protein

Figure 2 shows an ultra-thin Lowicryl section adjacent to the semi-thin section of Figure 1. The low-power micrograph of Figure 2A shows part of the ependymal thickening in the ventricular wall. A detail (framed area in Figure 2A) of the apical portion of the ependymal cells shows varicosities of the supra-ependymal plexus (arrowheads in Figure 2B), containing small dense-core vesicles (open arrow). B-50 immunoreactivity is found predominantly at the plasma membrane of the varicosities (arrowheads). Cilia (stars) show

Figure 4. (**A**,**B**) Electron micrographs of ultra-thin Lowicryl sections incubated with monoclonal antibodies to synaptophysin (p38) and 5-nm gold particles coupled to goat anti-mouse IgGs. The gold particles are silver enhanced to a diameter of 10 nm. Note the high immunoreactivity on and close to electron-lucent small synaptic vesicles, and absence of immunoreactivity in large dense-core vesicles (open arrows). G, glial cell process; Mit, mitochondrion. Bars = 0.5 µm.

Figure 5. Detail of a section through myelinated axons (MAx) and unmyelinated axons (Ax) in the MCG, incubated with antibodies to myelin basic protein (MBP) and 10-nm gold particles coupled to goat anti-rabbit IgGs. High immunoreactivity for MBP is found in the compact myelin. Bar = 0.5 µm.

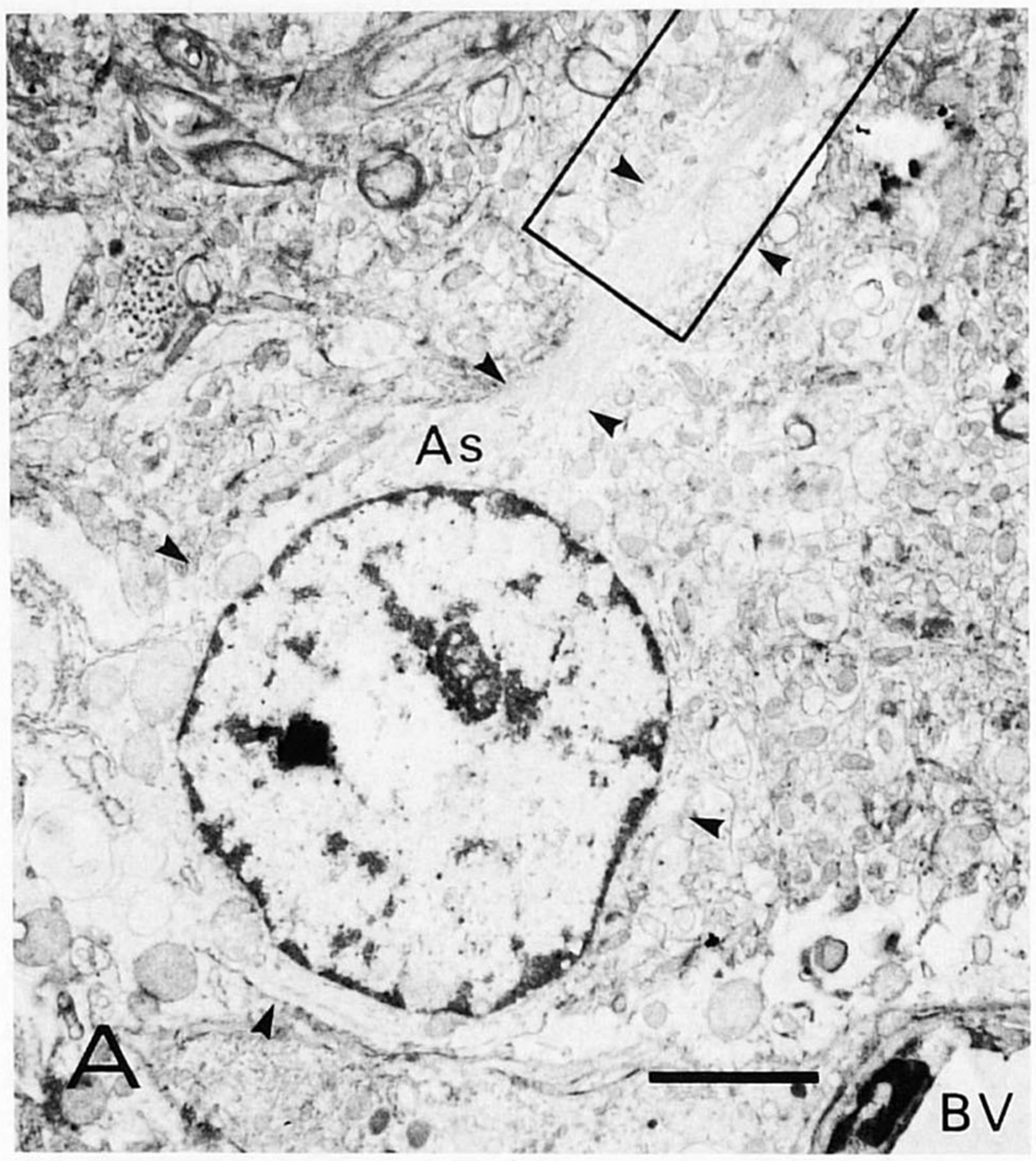
As
A
BV

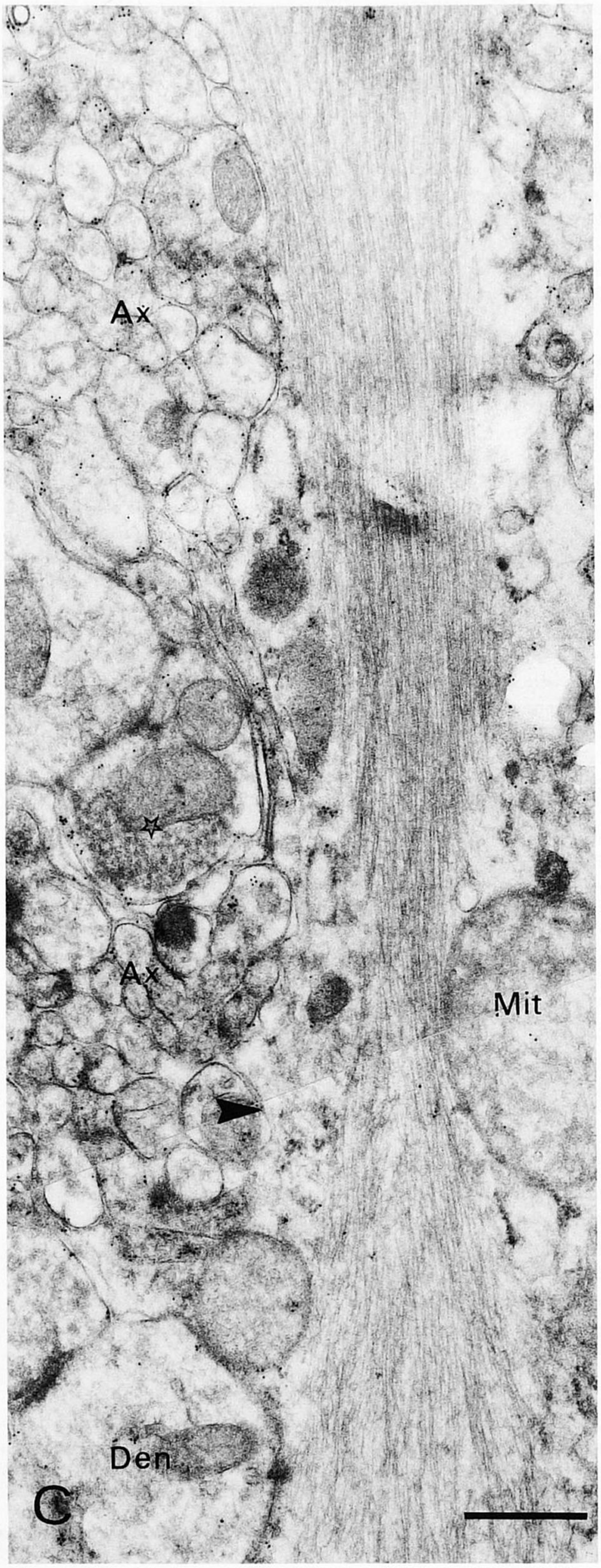
Ax
Ax
Mit
Den
C

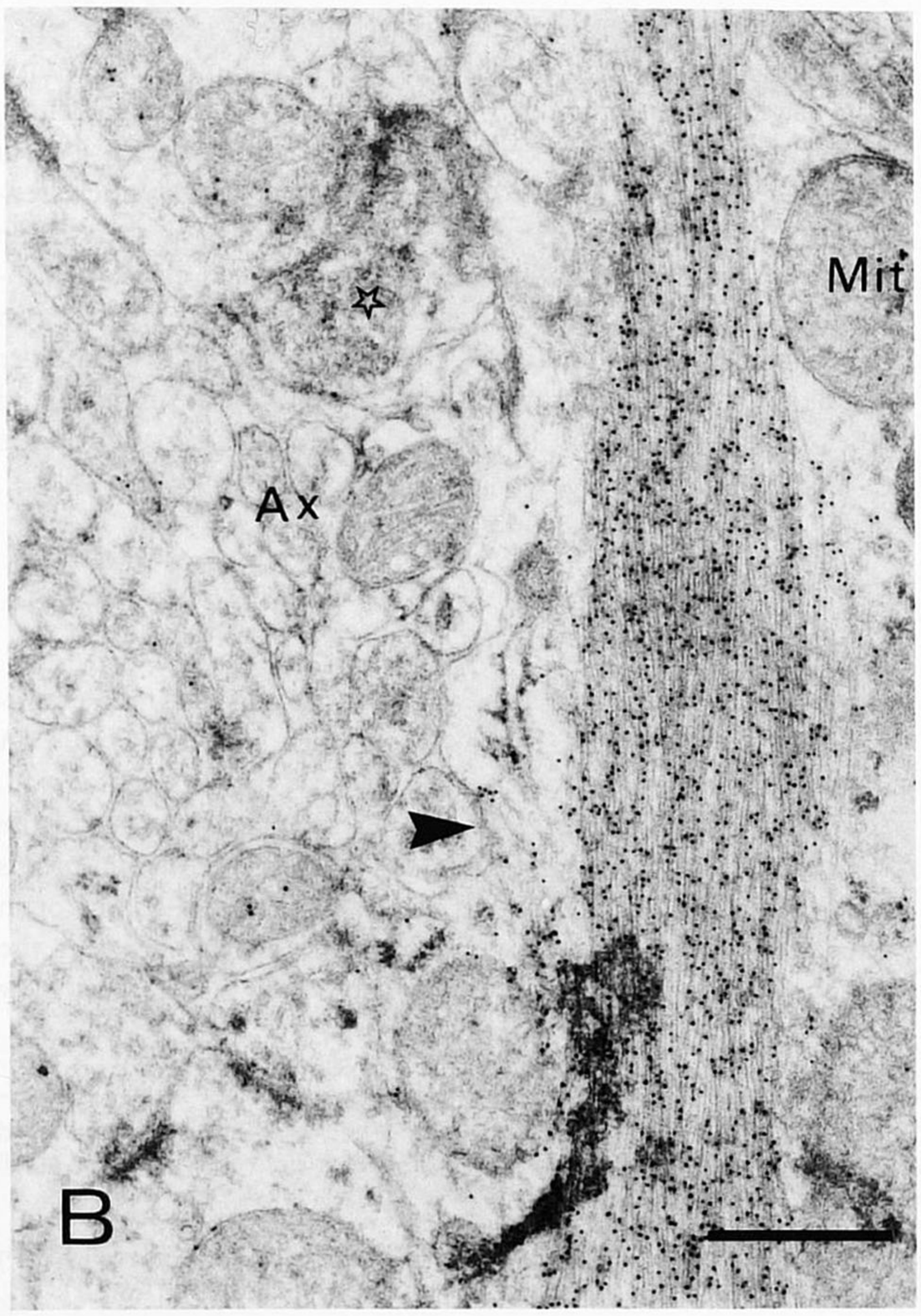
Mit
Ax
B

low B-50 immunoreactivity, slightly above background, and the apical plasma membrane of ependymal cells (curved arrows) is without B-50 immunoreactivity. Figure 2C gives a detail of the subependymal layer, in which axons are sectioned longitudinally. B-50 is present mainly at the plasma membrane of the unmyelinated small axons (Ax). In the basolateral region of the MCG, more distant from the aqueduct, axon varicosities (star in Figure 3A; Figure 3B gives a detail of Figure 3A), bundles of small unmyelinated axons (Ax) and dendrites (Den) are found. The varicosities contain either small electron-lucent synaptic vesicles (SSV, open star) or both electron-lucent and large dense-core vesicles (DCV, closed stars). Note the high density of B-50 immunoreactivity at the plasma membrane of the cross-sectioned small unmyelinated axons. The axon varicosities show B-50 immunoreactivity both at the plasma membrane and in the cytosol, whereas the plasma membrane of dendrites is virtually without B-50 immunoreactivty. The plasma membrane forming the presynaptic part of the synaptic junction (between curved arrows; Figure 3B) also appears to be without B-50 immunoreactivity. High synaptophysin immunoreactivity is found in areas of varicosities which are filled with small electron-lucent synaptic vesicles (Figures 4A and 4B). Only background immunolabeling is found over mitochondria (Mit) and glial protrusions (G). Note the absence of synaptophysin immunoreactivity at large dense-core vesicles (open arrows).

MBP is a basic membrane protein present in compact myelin of the rat CNS. Antibodies clearly detect MBP in the myelin surrounding the axons (MAx, Figure 5). Virtually no immunolabeling is found over unmyelinated axons (Ax). Note the absence of immunoreactivity in the internal mesaxon of the lower right MAx.

Comparison of the Ultrastructural Localization of B-50 with Glial Fibrillary Acidic Protein and Adrenocorticotropic Hormone

Serial sections were incubated with antibodies to B-50 and to GFAP to determine whether B-50 is present in astrocytes of mature brain. Large ultra-thin sections had to be prepared in order to obtain a section of the MCG containing one of the sparsely distributed astrocytes and its processes. Figure 6A shows a low-power photomicrograph of an astrocyte (As, surroundings indicated with small arrowheads) adjacent to a blood vessel (BV). The framed area is shown at higher magnification in Figure 6C. Figures 6B and 6C show details of the astrocyte process and surrounding neuropil in two serial sections immunoreacted for GFAP and B-50, respectively. The arrowhead indicates a corresponding position in both sections. Note the fine structural preservation of the glial intermediate filaments, which are highly immunoreactive for GFAP (Figure 6B). B-50 is virtually absent from the plasma membrane of the astrocyte cell body and the astrocyte process (Figure 6C), whereas the plasma membranes of the surrounding small unmyelinated axons (Ax) show a high density of B-50 immunoreactivity.

The MCG is innervated by ACTH-containing varicosities derived from axon extensions of neurons in the arcuate nucleus (3,39). The number of ACTH varicose profiles in the ventromedial region of the MCG is relatively low, and large sections are therefore needed to trace the few profiles. Figure 7A shows a varicosity that has been immunoreacted with an antiserum directed against the amino acid sequence 25–39 of the ACTH molecule. Immunoreactivity, as shown by 10-nm gold particles coupled to GAR-IgGs, is located close to large dense-core vesicles in the varicosity and is absent from the small electron-lucent vesicles (open arrowhead), in accordance with former studies (3,39). In line with former biochemical studies on the interaction of ACTH with B-50 phosphorylation (46), we were interested in the relative distribution of these two molecules in the rat MCG. To label both ACTH and B-50 in the same section, we silver enhanced the gold particles that visualize ACTH [25–39] immunoreactivity. With this silver enhancement procedure it is possible to prevent any crossreaction between antibodies and gold-coupled IgGs applied to detect ACTH, and the primary and secondary antibodies used to detect B-50 (1,39). In Figure 7B one of our results is presented, demonstrating the differential location of B-50 (10-nm gold particles) and ACTH (40–80-nm silver-enhanced gold particles), present at the plasma membrane and at dense-core vesicles, respectively.

Discussion

The main goal of our study was to find a suitable preparation method with which we could perform immunogold localization studies of B-50 and could relate the localization of this protein with that of other neural proteins. The controls indicate that the immunoreactivity of the various antibodies with the homologous antigens in the Lowicryl HM20 sections is highly specific. As we have illustrated, the method of Lowicryl HM20 embedding after freeze-substitution offers the advantage of the application of conventional sectioning techniques at room temperature in combination with post-embedding immunogold labeling. The good sectioning properties of Lowicryl HM20 are mainly due to the non-polar nature of the resin. During sectioning there is no spreading of the section on the water surface in the trough, as observed with the polar Lowicryl K4M (30). With Lowicryl HM20-embedded brain tissue it is possible to process large silver or silver-gray serial sections and trace sparse cell structures (Figures 6 and 7). In addition to these advantages of the Lowicryl HM20 resin, the hydrophobic nature of the resin and the smooth surface of the section appear to reduce label efficiency compared with ultra-thin cryosections (18). Immunogold labeling procedures on cryosections of glutaraldehyde-fixed rat brain (41) resulted in a higher label density for B-50. However, in cryosec-

Figure 6. (**A**) Low-power micrograph of an astrocyte (As, contours marked with arrowheads) in the ventromedial MCG adjacent to a blood vessel (BV), showing the well-preserved morphology of the astrocyte cell body, its processes, and the surrounding neuropil. (**B,C**; framed area in **A**) Two serial sections of this astrocyte, immunoreacted with antibodies to GFAP and B-50, respectively, visualized with 10-nm gold particles. Note the preservation of the intermediate filaments filing the central region of the astrocyte process and high immunoreactivity of these filaments for GFAP. Arrowhead marks identical position in both sections. B-50 is present at the plasma membrane of unmyelinated axons (Ax) and varicosities, but absent from that of the astrocyte process. Den, dendrite; Mit, mitochondrion. Bars: **A** = 5 μm; **B,C** = 0.5 μm.

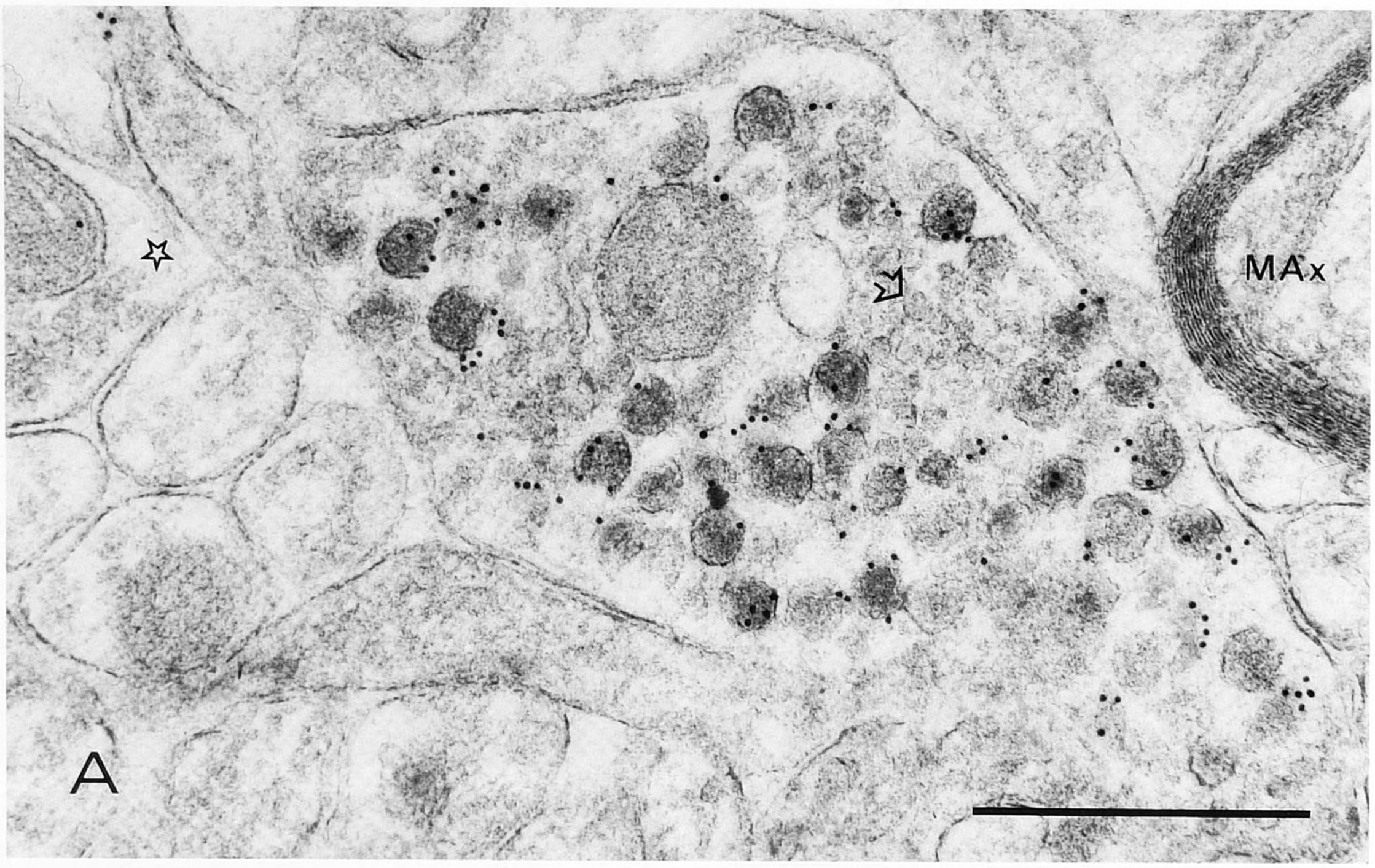
MAx
A

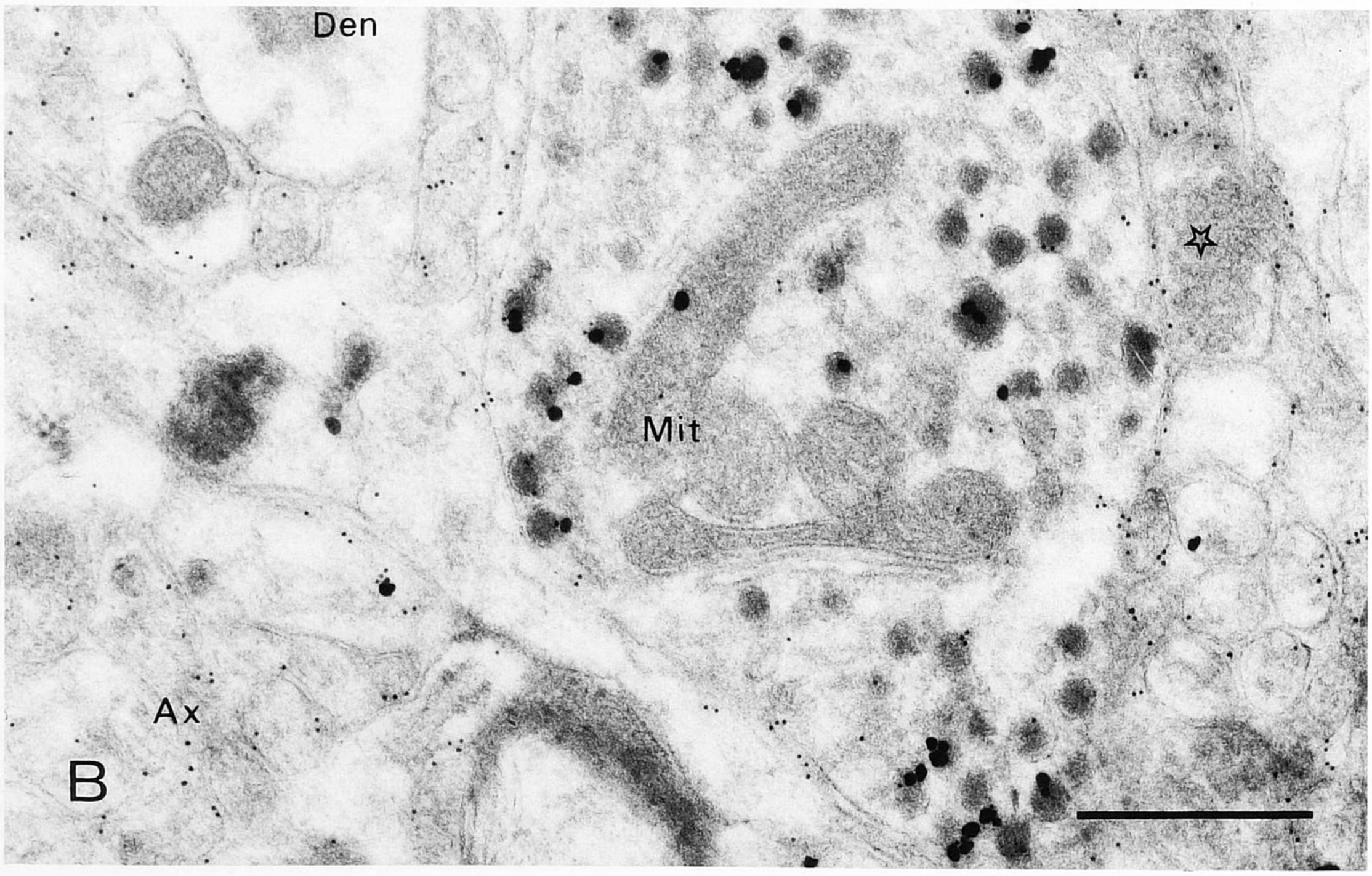
Den
Mit
Ax
B

tions of the MCG, ACTH immunoreactivity was not found in large dense-core vesicles but spread in and around the varicosities, probably due to solubilization of cell components during treatment of the cryosections (unpublished results).

Dehydration with methanol by dissolving the ice at very low temperatures, as performed in this study, may account for the good retention of ultrastructure and antigenicity. Adding uranyl acetate to the freeze-substitution medium further prevents loss of lipids during dehydration and resin embedding (43,44). In comparison, dehydration with the PLT method starts at 0°C, replacing the liquid waters and thus causing less retention of ultrastructure and antigenicity (13). The limitation of both methods may be the chemical pre-fixation of the tissue. Chemical pre-fixation can be avoided by cryofixing the specimen followed by freeze-substitution and low-temperature embedding (12,15,17,18,32,36,38). Cryofixation instantaneously arrests biological processes and preserves the structure (11). However, cryofixation of tissues causes ice crystal formation and thus distortion of ultrastructure in deeper layers (36,38). This is a disadvantage when observations over a wide area of tissue are necessary to detect sparsely distributed structures. Improvement of cryofixation in tissues has recently been successul with the high-pressure freezing method, in which expansion of ice crystals is prevented by using high pressure during the freezing process (14,20,21,28,34).

Subcellular Localization of B-50

B-50 (also termed GAP43, GAP48, F1, pp46, neuromodulin) is a neural phosphoprotein which is expressed at high levels in outgrowing neurites (33). In synaptosomes isolated from mature rat cortex, B-50 plays an important role in the release of norepinephrine, suggesting a role in neurotransmission (9). From our ultrastructural localization studies, it is clear that the location of B-50 is not confined to the axon terminal but is present along the entire axolemma of bundles of unmyelinated axons and varicosities, suggesting local functions in this region of the axon (40). B-50 has long been characterized as a neuron-specific protein. However, recently B-50 was detected immunocytochemically and biochemically in cultures of glial O-2A progenitor cells (10) and mature fibrous astrocytes and oligodendrocytes (8). It is still an open question whether B-50 is expressed in glial cells in situ of the developing central nervous system of the rat. In situ studies on this issue have not yet been reported. The evidence of glial B-50 expression is limited to cultured glial cells. By the application of ultra-thin serial sections, it was possible to find sparsely distributed astrocytes in MCG and to demonstrate that in the MCG of adult rats B-50 is not present in the cell bodies and processes of astrocytes, identified by their content of GFAP-immunoreactive filaments (29). Moreover, in oligodendrocytes of the MCG we found no B-50 immunoreactivity (results not shown). This study shows that the method of freeze-substitution of CNS and low-temperature embedding in HM20 can be applied to more extended studies on the developmental expression of B-50 in glial cells.

The fair preservation of ultrastructure in the ultra-thin Lowicryl HM20 sections allows double labeling procedures combined with silver enhancement. The primary and secondary antibodies applied to detect ACTH can be inactivated by means of silver enhancement (1). We took advantage of this procedure to study simultaneously the localization of B-50 and ACTH in axon varicosities. The silver enhancement of gold particles recognizing ACTH antibodies made it possible to trace the sparse varicosities at low magnification in the electron microscope. As illustrated (Figure 7), the ultrastructure remains intact and the antigenicity for B-50 persists, being present predominantly at the plasma membrane.

Detection of Other Neural Antigens

The ultrastructure of the myelin sheathes is well preserved and so is that of the mesaxon and the microtubules in the axon. The antiserum to MBP gives a specific staining of the compact myelin, in accordance with immunocytochemical ultrastructural studies of others (31). The background gold labeling appears to be very low.

Another example is the detection of synaptophysin, also referred to as protein p38. This protein has been identified as a major integral membrane glycoprotein of neuronal small synaptic vesicles and of related small clear vesicles in neuroendocrine cells (16,23,45). In this study, immunogold labeling on HM20 sections showed that synaptophysin was found in axon terminals filled with small electron-lucent synaptic vesicles, whereas the large dense-core secretory granules showed virtually no immunoreactivity.

In conclusion, we have developed a procedure of freeze-substitution and low-temperature embedding of neural tissue in Lowicryl HM20. The well-preserved ultrastructure and antigenicity for a variety of proteins, together with the good sectioning properties of the Lowicryl HM20 resin, make this method suitable for ultrastructural multiple-immunolabeling studies.

Acknowledgments

We wish to thank Etienne R.A. Jap Tjoen San for writing the quantification program and Jacob B.I. Rousseau for constructive suggestions, Ruud J. Bloemen for affinity purification of the B-50 antibodies, and Dr A.A.J. Verhofstad for the gift of anti-ACTH[25–39] antiserum.

Literature Cited

1. Bienz K, Egger D, Pasamontes L: Electron microscopic immunocytochemistry. Silver enhancement of colloidal gold marker allows double labeling with the same primary antibody. J Histochem Cytochem 34:1337, 1986
2. Buma P: Synaptic and nonsynaptic release of neuromediators in the CNS. Acta Morphol Neerl Scand 26:81, 1989
3. Buma P, Veening J, Nieuwenhuys R: Ultrastructural characterizaiton of adrenocorticotrope hormone (ACTH) immunoreactive fibres in the

Figure 7. (**A**) Ultra-thin Lowicryl section of a cross-sectioned fiber bundle, containing a varicosity filled with dense-core secretory granules. The section is incubated in antibodies to ACTH[25–39] and second antibodies coupled to 10-nm gold particles. Only large dense-core vesicles are labeled for the neuropeptide. Small electron-lucent synaptic vesicles (open arrow and star) are devoid of ACTH immunoreactivity. The section shown in **B** was treated as described for **A**. Gold particles were silver enhanced to yield a diameter of 40–80 nm. Subsequently, the section was re-immunoincubated in anti-B-50 antibodies and 10-nm gold coupled to GAR-IgGs. High B-50 immunoreactivity is found at the axolemma of cross-sectioned axons surrounding the ACTH-immunoreactive varicosity. Bars = 0.5 μm.

mesencephalic central gray substance of the rat. Eur J Neurosci 1:659, 1989

4. Carlemalm E, Garavito RM, Villiger W: Resin development for electron microscopy and an analysis of embedding at low temperature. J Microsc 126:123, 1982
5. Carlemalm E, Villiger W, Acetarin JD, Kellenberger E: Low temperature embedding. In Müller M, Becker RP, Boyde RP, Wolosewick JJ, eds. The science of biological specimen preparation 103. AMF O'Hare, IL, SEM Inc, 1986, 147
6. Celio MR, Keller GA, Bloom FE: Immunoelectronmicroscopy of neural antigens on ultrathin frozen sections. J Histochem Cytochem 34:491, 1986
7. Chatelain B, Dupouy JP, Dubois MP: Ontogenesis of cells producing polypeptide hormones (ACTH, MSH, LPH, GH, prolactin) in the fetal hypophysis of the rat; influence of the hypothalamus. Cell Tissue Res 196:409, 1979
8. Cunha A, Vitkovic L: Regulation of immunoreactive GAP-43 expression in rat cortical macroglia is cell type specific. J Cell Biol 111:209, 1990
9. Dekker LV, De Graan PNE, Versteeg DHG, Oestreicher AB, Gispen WH: Phosphorylation of B-50 (GAP43) is correlated with neurotransmitter release in rat hippocampal slices, J Neurochem 52:24, 1989
10. Deloulme J-C, Janet TH, Au D, Storm D, Sensenbrenner M, Baudier J: Neuromodulin (GAP43): a neuronal protein kinase C substrate is also present in O-2A glial cell lineage. Characterization of neuromodulin in secondary cultures of oligodendrocytes and comparison with the neuronal antigen. J Cell Biol 111:1559, 1990
11. Heuser JE, Reese TS, Dennis MJ, Jan Y, Jan L, Evans L: Synaptic vesicle exocytosis captured by quick freezing and correlated with quantal transmitter release. J Cell Biol 81:275, 1979
12. Humbel B, Marti T, Müller M: Improved structural preservation by combining freeze substitution and low temperature embedding. Beitr Elektronmikros Direktabb Oberfl 16:585, 1983
13. Humbel B, Schwarz H: Freeze-substitution for immunochemistry. In Verkleij AJ, Leunissen JLM, eds. Immunogold labeling in cell biology. Boca Raton, FL, CRC Press, 1989, 115
14. Hunziker EB, Herrmann W: In situ localization of cartilage extracellular matrix components by immunoelectron microscopy after cryotechnical tissue processing. J Histochem Cytochem 35:647, 1987
15. Ichikawa M, Sasaki K, Ichikawa A: Immunocytochemical localization of amylase in gerbil salivary gland acinar cells processed by rapid freezing and freeze-substitution fixation. J Histochem Cytochem 37:185, 1989
16. Jahn R, Schiebler W, Ouimet C, Greengard P: A 38,000-dalton membrane protein (p38) present in synaptic vesicles. Proc Natl Acad Sci USA 82:4137, 1985
17. Kellenberger E, Carlemalm E, Villiger W: Physics of the preparation and observation of specimens that involve cryoprocedures. In Müller M, Becker RP, Boyde RP , Wolosewick JJ, eds. The science of biological specimen preparation, 103. AMF O'Hare, IL, SEM, Inc, 1986, 147
18. Kellenberger E, Dürrenberger M, Villiger W, Carlemalm E, Wurtz M: The efficiency of immunolabel on Lowicryl sections compared to theoretical predictions. J Histochem Cytochem 35:959, 1987
19. Merighi A, Polak JM, Fumagalli G, Theodosis DT: Ultrastructural localization of neuropeptides and GABA in rat dosal horn: a comparison of different immunogold labeling techniques. J Histochem Cytochem 37:529, 1989
20. Moor H: Theory and practice of high pressure freezing. In Steinbrecht RA, Zierold K, eds. Cryotechniques in biological electron microscopy. Heidelberg, Springer-Verlag, 1987, 175
21. Moor H. Bellin G: The influence of high pressure freezing on mammalian nerve tissue. Cell Tissue Res 209:201, 1980
22. Müller M, Marti T, Kriz S: Improved structural preservation by freeze substitution. In Brederoo P, De Priester W, eds. Electron microscopy, 1980. Proc 7th Eur Congr Electron Microsc, 2. The Hague, 720
23. Navone F, Jahn R, DiGioia G, Stukenbrok H, Greengard P, De Camilli P: Protein p38: an integral membrane protein specific for small vesicles of neurons and neuroendocrine cells. J Cell Biol 103:2511, 1986
24. Oestreicher AB, Gispen WH: Comparison of the immunocytochemical distribution of the phosphoprotein B-50 in the cerebellum and hippocampus of immature and adult rat brain. Brain Res 375:267, 1986
25. Oestreicher AB, Van Dongen CJ, Zwiers H, Gispen WH: Affinity-purified anti-B-50 protein antibody: interference with the function of the phosphoprotein B-50 in synaptic plasma membranes. J Neurochem 41:331, 1983
26. Paxinos G, Watson C: The rat brain in stereotaxic coordinate. New York, Academic Press, 1982
27. Reynolds ES: The use of lead citrate at high pH as an electron-opaque stain in electron microscopy. J Cell Biol 17:208, 1963
28. Riehle U: Schnellgefrieren organischer Präparate für die Elektronen-Mikroskopie. Chem Ing Tech 40:213, 1968
29. Schachner M, Hedley–Whyte ET, Hsu DW, Schoonmaker G, Bignami A: Ultrastructural localization of glial fibrillary acidic protein in mouse cerebellum by immunoperoxidase labeling. J Cell Biol 75:67, 1977
30. Schwarz H, Humbel B: Influence of fixatives and embedding media on immunolabelling of freeze-substituted cells. Scanning Microsc (supp)3:57, 1989
31. Schwob VS, Clark BH, Agrawal D, Agrawal HC: Electron microscopic immunocytochemical localization of myelin proteolipid protein and myelin basic protein to oligodendrocytes in rat brain during myelination. J Neurochem 45:559, 1985
32. Sitte H, Neumann K, Edelmann L: Cryosubstitution for routine work in transmission electron microscopy. In Müller M, Becker RP, Boyde RP, Wolosewick JJ, eds. The science of biological specimen preparation. AMF O'Hare, IL, SEM, Inc, 1986, 103
33. Skene JHP: Axonal growth-associated proteins. Annu Rev Neurosci 12:127, 1989
34. Studer D, Michel M, Müller M: High pressure freezing comes of age. Scanning Microsc (supp)3:253, 1989
35. Tramu G, Dubois MP: Comparative cellular localization of corticotropin and melanotropin in lerot adenohypophysis (Eliomys quercinus). Cell Tissue Res 183:457, 1977
36. Usuda N, Ma H, Hanai T, Yokota S, Hashimoto T, Nagata T: Immunoelectron microscopy of tissues processed by rapid freezing and freeze-substitution fixation without chemical fixatives: application to catalase in rat liver hepatocytes. J Histochem Cytochem 38:617, 1990
37. Valentino KL, Crumrine DA, Reichardt LF: Lowicryl K4M embedding of brain tissue for immunogold electron microscopy. J Histochem Cytochem 34:969, 1986
38. Van Harreveld A, Crowell J, Malhotra, SK: A study of extracellular space in central nervous tissue by freeze substitution. J Cell Biol 25:117, 1965
39. Van Lookeren Campagne M, Oestreicher AB, Buma P, Verkleij AJ, Gispen WH: Ultrastructural localization of B-50/GAP43 and adrenocorticotrope hormone (ACTH) in Lowicryl HM20 embedded rat mesencephalic central gray area. Neuroscience 42:517, 1991
40. Van Lookeren Campagne M, Oestreicher AB, De Graan P, Gispen WH: The role of B-50 in nerve growth cone function. In Kater SB, Letourneau PC, Macagno ER, eds. The nerve growth cone. New York, Raven Press, 1992, 97
41. Van Lookeren Campagne M, Oestreicher AB, Van Bergen en Henegouwen PMP, Gispen WH: Ultrastructural double localization of B-50/GAP43 and synaptophysin (p38) in neonatal and adult rat hippocampus. J Neurocytol 19:948, 1990

42. Van Lookeren Campagne M. Oestreicher AB, Van Bergen en Henegouwen PMP, Gispen WH: Ultrastructural immunocytochemical localization of B-50/GAP43, a protein kinase C substrate, in isolated presynaptic nerve terminals and neuronal growth cones. J Neurocytol 18:479, 1989

43. Verkleij AJ, Humbel B, Studer D, Müller M: 'Lipidic particle' systems as visualized by thin-section electron microscopy. Biochim Biophys Acta 812:591, 1985

44. Weibull C, Christiansson A, Carlemalm E: Extraction of membrane lipids during fixation, dehydration and embedding of Acholeplasma laidlawii-cells for electron microscopy. J Microsc 129:201, 1983

45. Wiedenmann B, Franke WW: Identification and localization of synaptophysin, an integral membrane glycoprotein of Mr 38,000 characteristic of presynaptic vesicles. Cell 41:1017, 1985

46. Zwiers H, Veldhuis HD, Schotman P, Gispen WH: ACTH-induced inhibition of endogenous rat brain phosphorylation *in vitro*: structure-activity. Neurochem Res 3:455, 1978